Electric Power Systems Research 216 (2023) 109017

Contents lists available at ScienceDirect

Electric Power Systems Research

journal homepage: www.elsevier.com/locate/epsr

Unified AC Transmission Expansion Planning Formulation incorporating VSC-MTDC, FACTS devices, and Reactive Power compensation

Ricardo A. de Araujo [a,*], Santiago P. Torres [b], José Pissolato Filho [a], Carlos A. Castro [a], Dirk Van Hertem [c]

[a] University of Campinas, Campinas, Brazil
[b] University of Cuenca, Cuenca, Ecuador
[c] KU Leuven University, Leuven, Belgium

ARTICLE INFO

Keywords:
HVDC
AC/DC model
FACTS
Reactive power compensation

ABSTRACT

The main aim of the static Transmission Network Expansion Planning (TNEP) is to determine which and where new transmission equipment must be installed. The complexity added by the non-linearities leads to simplifications, which include the DC model. However, most non-linearities are solvable nowadays. Thus, the new scenario of large non-dispatchable power sources penetration and the several developments in technologies, e.g, Flexible AC Transmission Systems (FACTS) devices and High Voltage Direct Current (HVDC) interconnections, motivate the use of the AC model with its non-linearities. Some research works address the use of some of those technologies for TNEP in an independent fashion, which can lead to sub-optimal solutions. In this work, Voltage Source Controlled-Multiterminal HVDC (VSC-MTDC) systems, FACTS devices, and Reactive Power Planning (RPP) are integrated into the same planning optimization process, so that a unified AC TNEP formulation is proposed. A non-linear mathematical programming technique and a differential evolution based metaheuristics are chosen to achieve an optimal transmission configuration. To evaluate the benefits of the proposed approach, two IEEE modified test systems (9 and 118 buses) are used. Results suggest that more economical solutions can be obtained if different types of reinforcement strategies are taken into account in a unified approach.

1. Introduction

Constant changes in electric systems introduce new challenges to the already complex TNEP problem [1,2]. The basic aim of the conventional static TNEP is to determine where and which new transmission reinforcements must be implemented. It is fundamental that both Kirchhoff's laws (linear form) in the DC model, presented in [3], are met throughout the system, which represents a relaxation of a complicated nonlinear programming problem. As a consequence of nonlinearity, intermediate models were developed, for example, the disjunctive linear model [4]. In that method, to overcome the non-linearity of Kirchhoff's second law, the nonlinear DC TNEP model is converted into the MILP (mixed-integer linear) model [5]. Ref. [6] proposes a resilient-constrained stochastic CGTEP (coordinated generation and transmission expansion planning) model including natural disasters, where an approximated linearized AC optimal power flow is adopted to represent the grid. Although the DC model is widely studied, its application in a practical system is not feasible [7,8]. Contrarily, using the AC model can produce several benefits, such as a simultaneous solution of the Reactive Power Planning (RPP) and the TNEP problems, high voltage direct current (HVDC) links, and FACTS devices modeling [9]. Additionally, it enables different studies after the TNEP step, for example, voltage stability analysis [10]. In [11], a simplified AC-DC TNEP model (disregarding the RPP) targeted to minimize investments, operational, and load shedding costs is proposed. In [12], an approximated AC modeling is implemented to simultaneously find the TNEP and the RPP requirements. A multi-period hybrid AC/DC TNEP formulation, including converter station equipment losses, and shunt compensation is proposed in [13].

As a consequence of power electronics advances, the availability of HVDC links and FACTS (Flexible AC Transmission System) devices has become a viable option, which demands the TNEP approaches to include equations in the formulations representing these new types of reinforcements [14–17]. In [18], a multistage robust TNEP model of ultrahigh-voltage AC/DC hybrid grids is proposed, incorporating the $N-1$ security criterion in the constraints. The work presented in [19]

* Corresponding author.
E-mail address: ricardoa@unicamp.br (R.A. de Araujo).

https://doi.org/10.1016/j.epsr.2022.109017
Received 5 October 2022; Received in revised form 13 November 2022; Accepted 20 November 2022
Available online 1 December 2022

Nomenclature

Set of

Ω	AC branches candidates.
Γ	DC branches candidates.
Υ	AC buses candidates to receive an SVC device.
Ψ	AC branches candidates to receive an TCSC device.
$\mathbb{B}$	All system buses (AC and DC).
$\mathbb{B}_{\mathbb{AC}}$	All AC buses.
$\mathbb{B}_{\mathbb{PQ}}$	All PQ buses.
$\mathbb{B}_{\mathbb{G}}$	All generator buses.
$\mathbb{B}_{\mathbb{C}}$	All AC buses with linked AC/DC converters.
$\mathbb{B}_{\mathbb{D}}$	All DC buses with linked AC/DC converters.
$\mathbb{B}_{\mathrm{SVC}}$	All buses with linked SVC device.
$\mathbb{R}$	All branches (AC and DC).
$\mathbb{R}_{\mathbb{AC}}$	All AC branches.
$\mathbb{R}_{\mathbb{DC}}$	All DC branches.
$\mathbb{R}_{\mathrm{TCSC}}$	All branches with linked TCSC device.

Parameters

r, b	Line resistance and reactance, respectively.
c_{VSC}	Fixed cost to install a new VSC converter.

Functions

ν	Total investment of the expansion.
χ	Total load shedding costs.
C_{SVC}, C_{TCSC}	Costs associated with SVC and TCSC devices respectively.

Binary Variables

γ, υ	Indicates whether or not a new DC circuit exists, indicate whether or not a new converter exists respectively.

Integer Variable

η	Number of new AC lines.

Continuous Variables

α	Active load shedding costs.
β	Reactive load shedding costs.
ρ	Active load shedding.
ϱ	Reactive load shedding.
G	Conductance matrix.
B	Susceptance matrix.
S	Apparent power.
P_{AC}, P_g, P_d	Active power: injection, generation, and load respectively.
Q_{AC}, Q_g, Q_d	Reactive power: injection, generation, and load respectively.
I_C	Converter current (AC side).
I	Electric current.
θ	Voltage phase angle.
U	Voltage magnitude.
U_C, U_{DC}	Voltage magnitude: at bus C and at DC bus respectively.
P_C, P_{DC}	Active power (converter station) — on AC side and on DC side, respectively.
P_{loss}	Losses — converter station.
Q_C	Reactive power injection (converter station) — on AC side.
B_{SVC}	SVC susceptance.
X_{TCSC}	TCSC reactance.
$X_{effective}$	Effective reactance of the line.
Q_{SVC}	SVC — reactive power generation.
Q_S	SVC — operating range.
Q_T	TCSC — operating range.

Indices

$\square^{max}, \square^{min}$	Maximum and minimum value respectively.
$\square_i$	At bus i.
$\square_{ij}$	Between buses $i-j$, $i \neq j$.

introduced a strategy to solve the multistage security-constrained TNEP problem, including AC and HVDC alternatives. Additionally, the model comprises some modified power flow equations to linearize the problem, which includes transmission losses using a piecewise linearization. A multi-objective expansion problem, considering HVDC, is presented in [20]. In [21], the stochastic TNEP in the presence of wind farms is proposed. The authors use the AC model and consider uncertain load and wind source conditions when reliability and N − 1 contingency is taken into consideration. FACTS devices into the TNEP problem are considered in [22]; nonetheless, the problem was linearized and modeled as MILP (mixed-integer linear programming). Most of the research works considered DC lines, FACTS devices, or shunt compensation in different formulations, which can lead to obtaining sub-optimal solutions. Therefore, by considering the three possibilities simultaneously, it is possible to achieve the optimal mix of the appropriate technologies, which represents an important and complex issue not treated in the literature.

Thus, considering all state-of-art summarized in Table 1, this research work proposes a unified AC-TNEP model, with the following transmission elements into the same optimization process: (i) VSC-MTDC devices, (ii) two different FACTS devices: (a) Static VAR Compensator (SVC) and (b) Thyristor Controlled Series Compensator (TCSC), and (iii) reactive power planning. A hybrid mathematical programming technique is used in conjunction with the differential evolution technique to solve the static planning model. It is crucial to highlight that the relevance of this work does not refer to TNEP solution techniques, but rather to show the feasibility of using a complete AC model with different system reinforcements possibilities in the same optimization process.

This work is structured in five sections, including the introduction and conclusion sections. The second section presents the models referring to the AC and DC grids, the two different FACTS devices used, in addition to the model of the VSC converter. In the following section, the work discusses the mathematical modeling and solution method. In Section 4, the results are discussed.

2. System modeling

2.1. AC grid

For this grid, the AC power flows are modeled by nonlinear equations, which are functions of nodal voltages and the system's topology. Operating constraints are included to characterize the real conditions of the grid - e.g., voltage limits for each bus, and power flow limits. The power injections at node i are determined as:

$$P_{AC_i} = U_i \sum_{j \in M_i} U_m [G_{ij} \cos(\theta_i - \theta_j) + B_{ij} \sin(\theta_i - \theta_j)], \quad (1)$$

Table 1
Taxonomy of research works.

Reference	Linearized AC model	Full AC model	RPP	FACTS	AC lines	DC lines	VSC converters
[1,2]	✓						
[6]	✓			✓			
[9,10]		✓	✓				
[12]	✓		✓				
[13]	✓		✓		✓	✓	✓
[14]		✓		✓			
[15,17]		✓				✓	✓
[20]		✓			✓	✓	✓
[21]		✓	✓		✓		
[22]	✓			✓			
Proposed approach		✓	✓	✓	✓	✓	✓

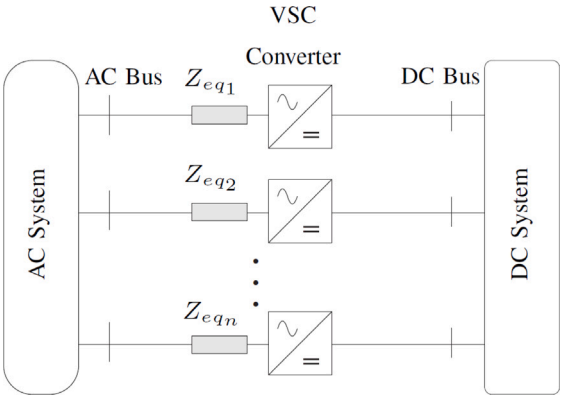

Fig. 1. AC/DC grid.

$$Q_{AC_i} = U_i \sum_{j \in M_i} U_m [G_{ij} \sin(\theta_i - \theta_j) - B_{ij} \cos(\theta_i - \theta_j)], \tag{2}$$

Thus, the power balances at bus i are:

$$P_{AC_i} = P_{gen_{AC_i}} - P_{load_{AC_i}}, \tag{3}$$

$$Q_{AC_i} = Q_{gen_{AC_i}} - Q_{load_{AC_i}}, \tag{4}$$

A detailed and complete analysis of these equations is available in [23,24].

2.2. DC grid

The DC grid presents only resistive components, and the power injection at node i is:

$$P_{DC_i} = 2U_{DC_i} \sum_{j \in \Psi_i} \frac{(U_{DC_i} - U_{DC_j})}{r_{ij}}, \tag{5}$$

Thus, the power balance must satisfy:

$$P_{DC_i} = P_{gen_{DC_i}} - P_{load_{DC_i}} \tag{6}$$

2.3. VSC converter

In this work, it is considered that n VSCs connect one AC grid to one MTDC grid, Fig. 1. Additionally, each converter has an equivalent impedance Z_{eq}, formed by a coupling transformer Z_{tf}, phase reactors Z_C and a filter Z_{filter}, illustrated in Fig. 2. Two crucial buses are linked to each converter (AC side); bus F is necessary to connect the AC filter, and bus C is the converter terminal. This work assumes the filter Z_{filter} can be omitted when adopting the modular multi-level converter (MMC) [25].

The power balance in each converter is given by:

$$P_C + P_{DC}^C + P_{loss} = 0 \tag{7}$$

Power losses are included to ensure the power balance, which is calculated through a general quadratic function that depends on the converter current (I_C), as shown below.

$$P_{loss} = a + bI_C + cI_C^2 \tag{8}$$

The coefficients a, b and c, and a full discussion of (8) is available in [26]. The converter current is given by:

$$I_C = \frac{\sqrt{P_C^2 + Q_C^2}}{\sqrt{3}U_C}, \tag{9}$$

The VSC presents the following voltage relationship between the two sides:

$$U_C^{max} = k_V \cdot U_{DC} = 1.1 \cdot U_{DC} \tag{10}$$

According to [27], k_V can be set to 1.1 pu (maximum) if no overmodulation is required.

2.4. FACTS devices

Usually, the maximum power transfer through transmission lines is increased by adding new transmission circuits. However, the installation of new transmission lines can be undesirable due to planning constraints. Thus, to avoid major additions to the existing system, it is possible to use appropriate FACTS devices to increase power transfer. This work uses two FACTS devices: (i) thyristor-controlled series compensator, and (ii) static VAR compensator. A detailed description of these two FACTS devices can be found in the Refs. [28–32].

2.4.1. Static VAR Compensator — SVC

Static Var Compensators are devices to compensate for the reactive power at points in the system, thus regulating the voltage and collaborating with the dynamic stability of the grid [28]. Thus, according to [28,33], if the reactive load is:

(i) capacitive, the SVC will use reactors (generally Thyristor Controlled Reactors) to consume the VARs from the grid, decreasing the grid voltage;
(ii) inductive, the capacitors are switched in, increasing the grid voltage.

The SVC can be treated as a variable susceptance, as shown in Fig. 3.

Therefore, the reactive power injection by SVC is defined by (11), indicating the strong relationship between reactive power flux and voltage magnitude.

$$Q_{SVC} = -U^2 B_{SVC}, \tag{11}$$

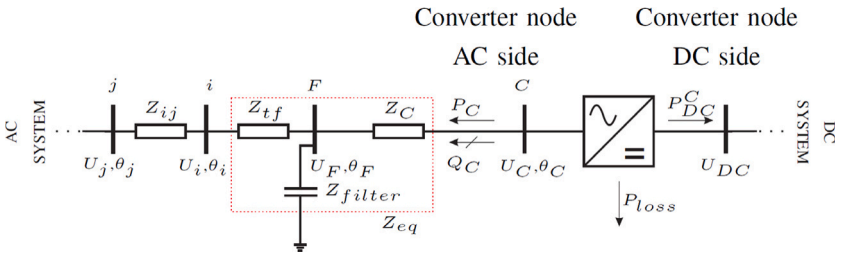

Fig. 2. VSC station model.

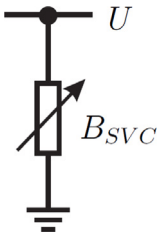

Fig. 3. SVC variable susceptance model.

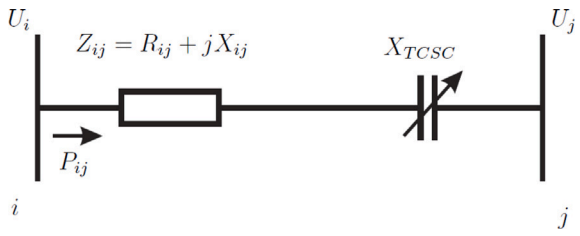

Fig. 4. Model — TCSC in a transmission line.

2.4.2. Thyristor Controlled Series Compensator — TCSC

The TCSC is a capacitive reactance compensator connected in series with the transmission line. According to [30], the TCSC is incorporated into the transmission line model by simply adding the variable reactance X_{TCSC} to the base reactance X_{ij} of the line. The TCSC can modify the electrical length of the line by adding inductive or capacitive reactance. Thus, the changes in line reactance, caused by the inclusion of the TCSC directly, impact the power flow of the line to which it is connected. The model of the transmission line with a TCSC connected between the buses $i-j$ is illustrated in Fig. 4.

Thus, the TCSC can modify the effective reactance of the line [29,30]:

$$X_{ij_{effective}} = X_{ij} + X_{TCSC}\,, \tag{12}$$

where X_{TCSC} is defined by

$$X_{TCSC} = k_{TCSC} X_{ij} \tag{13}$$

The variable k_{TCSC} is the working range of TCSC reactance.

3. Problem formulation

Among the possible investment plans, the one that presents the lowest cost and meets the operational constraints is considered the optimal plan. Therefore, it is essential that economic and operational issues are included in the same problem.

3.1. Operation problem: Constraints

Each possible transmission topology needs to be evaluated and must satisfy a group of equality and inequality constraints, as follows:

3.1.1. Equality constraints

To guarantee the power flow balance, the power flows associated with the VSC converters are incorporated, as defined in (14) and (15).

$$(P_{g_i} - P_{d_i} - P_i) + \rho_i + (P_{C_i} - P_{DC_i} - P_{loss_i}) = 0 \qquad \forall i \in \mathbb{B} \tag{14}$$

$$(Q_{g_i} + Q_{SVC_i} - Q_{d_i} - Q_i) + \varrho_i + Q_{C_i} = 0 \qquad \forall i \in \mathbb{B}_{\mathbb{AC}} \tag{15}$$

3.1.2. Inequality constraints

Inequality constraints are represented as follows.

$$\left|S_{g_i}^{min}\right| \le \left|S_{g_i}\right| \le \left|S_{g_i}^{max}\right| \qquad \forall i \in \mathbb{B}_{\mathbb{G}} \tag{16}$$

$$U_i^{min} \le U_i \le U_i^{max} \qquad \forall i \in \mathbb{B} \tag{17}$$

$$\left|S_{ij}^{min}\right| \le \left|S_{ij}\right| \le \left|S_{ij}^{max}\right| \qquad \forall (i,j) \in \mathbb{R} \tag{18}$$

$$\left|U_{C_i}^{max}\right| \le 1.1 \cdot \left|U_{DC_l}\right| \qquad \forall i \in \mathbb{B}_{\mathbb{C}},\ \forall l \in \mathbb{B}_{\mathbb{D}} \tag{19}$$

$$\left|S_{C_i}\right| = \sqrt{P_{C_i}^2 + Q_{C_i}^2} \le \left|U_{C_i} I_{C_i}^{max}\right| \qquad \forall i \in \mathbb{B}_{\mathbb{C}} \tag{20}$$

$$-k_Q S_{nom_i} \le Q_{C_i} \le [-b_{C_i}(U_{C_i}^{max})^2 + b_{C_i} U_{C_i}^{max} \left|U_{F_i}\right| \cos(\theta_{C_i} - \theta_{F_i})] \qquad \forall i \in \mathbb{B}_{\mathbb{C}} \tag{21}$$

$$Q_{SVC_i}^{min} \le Q_{SVC_i} \le Q_{SVC_i}^{max} \qquad \forall i \in \mathbb{B}_{\mathbb{SVC}} \tag{22}$$

$$\rho_{min_i} \le \rho_i \le \rho_{max_i} \qquad \forall i \in \mathbb{B}_{\mathbb{PQ}} \tag{23}$$

$$\varrho_{min_i} \le \varrho_i \le \varrho_{max_i} \qquad \forall i \in \mathbb{B}_{\mathbb{PQ}} \tag{24}$$

$$X_{TCSC_{ij}}^{min} \le X_{TCSC_{ij}} \le X_{TCSC_{ij}}^{max} \qquad \forall (i,j) \in \mathbb{R}_{\mathbb{TCSC}} \tag{25}$$

The minimum and maximum apparent power generation limits are represented by (16). The voltage range in all grid buses is specified in (17). Eq. (18) corresponds to the transmission line capacity limits. The voltage relationship between the buses with direct connection to the VSC converter is defined by (19). The constraint of VSC apparent power is determined by (20), and it depends on the maximum current limit through the VSC (I_C^{max}). The upper and lower reactive power limits for the VSC are shown in (21). Eq. (22) represents the reactive power generation limits of Static Var Compensator devices.

The idea is to obtain a transmission expansion plan that satisfies all operational requirements without any load shedding. The inclusion of active load shedding limits (23) and reactive load shedding limits (24) constraints is necessary to guarantee the problem is always feasible. Naturally, any load shedding will be heavily penalized in the objective function; thus, any plan that involves load shedding will be admitted as a poor-quality one. Finally, the TCSC reactance limits are represented in (25).

3.2. Operation problem: Objective function χ

The load shedding cost associated with each topology is defined by:

$$\min \chi = \sum_{i \in \mathbb{B}_{\mathbb{PQ}}} (\alpha \rho_i + \beta \varrho_i)\,, \tag{26}$$

where ϱ can be understood as a necessary shunt compensation to the grid. The load shedding is characterized and modeled by fictitious generators connected to the PQ buses.

The result of $\beta\varrho_i$ is always positive, independent of the type of compensation (inductive or capacitive). Thus, the coefficient β must be modeled according to the type of compensation [9]. Considering the operational perspective, it is clear that the best investment solution is the one that does not involve load shedding ($\chi = 0$) and must satisfy equations defined by (14)–(24). Conversely, a nonzero load shedding expresses that the expansion plan (new topology) cannot meet the operation constraints, which characterizes a non-viable choice.

3.3. The economic problem: Objective function ν

It is mandatory to evaluate the cost associated with each possible investment plan in economic terms; that is, the investment cost for adding the different devices to the grid. This work proposes the function χ (26) as a penalty into the objective function ν, as follows

$$\min \nu = \{ \sum_{(i,m)\in\Omega} \lambda_{im}\eta_{im} + \sum_{(r,s)\in\Gamma} [(\tau_{rs}\gamma_{rs}) + c_{VSC}(\upsilon_r + \upsilon_s)]\} + C_{SVC} + C_{TCSC} + \chi \tag{27}$$

η_{im}, corresponds to the quantity of new AC lines between nodes i and m. The existence of a new DC circuit between the r and s buses is defined by the binary variable γ_{rs}. When a new line is added, γ_{rs} is equal to 1, otherwise, γ_{rs} is 0. The costs related to the new AC and DC lines are λ_{im} and τ_{rs}, respectively. The binary variables υ_r and υ_s indicate whether a new converter has been added (binary 1) at DC buses r or s. Refs. [34,35] define the terms C_{SVC} and C_{TCSC} of (27).

$$C_{SVC} = \sum_{i\in Y} (0.0003Q_{S_i}^2 - 0.305Q_{S_i} + 127.38) \tag{28}$$

$$C_{TCSC} = \sum_{(i,j)\in\Psi} (0.0015Q_{T_{ij}}^2 - 0.713Q_{T_{ij}} + 153.75) \tag{29}$$

C_{SVC} and C_{TCSC} are in \$/kVAr.

The constraints associated with the economic problem are given by:

$$0 \le \eta_{im} \le \eta_{max} \quad \eta_{im}, \eta_{max} \text{ integer}$$
$$\gamma_{rs} \quad \text{binary}$$
$$\upsilon_r, \upsilon_s \quad \text{binary}$$

3.4. Solution method

It is essential to highlight that the core focus of this work is directly related to the AC TNEP formulation incorporating VSC-MTDC, FACTS devices, and reactive power planning. Thus, different optimization procedures can be considered suited to solving problems of this type efficiently. Therefore, this work uses one of these techniques, named Differential Evolution (DE). This technique has been shown to obtain successful results for combinatorial, complex problems [36]. In the power systems area, there are quite a few research works published in top journals, where DE was successfully applied [37,38].

3.4.1. Differential evolution

DE consists in the manipulation of an initial set of individuals representing candidate solutions (topologies). Over the generations (iterations), the candidate solutions undergo mutation and cross modifications, generating new candidate solutions. In the next step, a selection is performed, and the cycle is repeated. In this work, the implementation of DE followed precisely the steps and parameters (mutation factor is set to 0.7 and crossover rate to 0.6) adopted by the authors in [39]. The only difference is the decision vector, where x_{min} and x_{max} incorporate AC lines, DC links, and FACTS devices. The decision vector initialization is performed exactly as described in [39], where an initial population of N_p vectors (individuals) $x_{j,i}$ is randomly generated. Each vector has dimension n and uses the following rule:

$$x_{j,i,0} = x_{j,min} + (x_{j,max} - x_{j,min}) rand_{i,j}[0,1] \tag{30}$$

where $x_{j,min}$ and $x_{j,max}$ represents the initial electric grid topology, and the maximum number of reinforcements (including the existent circuits) for the jth component, respectively, and *rand* is a uniform random number between 0 and 1. In this work, x_{min} and x_{max} are defined by:

$$x_{min} = [x_{min_L}\ x_{min_{SVC}}\ x_{min_{TCSC}}] \qquad x_{max} = [x_{max_L}\ x_{max_{SVC}}\ x_{max_{TCSC}}]$$

where x_{min_L} represents the initial AC-DC circuits, $x_{min_{SVC}}$ and $x_{min_{TCSC}}$ represents the initial SVC and TCSC devices connected to the network. x_{max_L} are the maximum number of AC-DC circuits, $x_{max_{SVC}}$ corresponds to the maximum number of SVCs in each bus, and $x_{max_{TCSC}}$ indicates the maximum number of TCSCs on each branch.

Fig. 5(a) shows a hypothetical grid, in which there are two available right-of-ways to add AC circuits: (1–2), and (2–3); one alternative to create DC circuits: (2–3); one possibility to add a TCSC: (1–3); and one SVC can be connected to bus 3. Thus, x_{min} is [1, 1, 1, 0, 0, 0], which means that there is an initial line between buses 1–2, buses 1–3, and nodes 2–3. x_{max} is [2, 1, 2, 1, 1, 1], indicating the maximum reinforcements allowed in the system. Fig. 5(b) illustrates the vectors x_{min} and x_{max}.

3.4.2. Implementation issues

Three computational tools are used to solve the TNEP problem. The *MATLAB* software [40] is used for data preparation and implementation of the differential evolution algorithm. For the operational problem, the (*AMPL*) environment [41], and the *KNITRO* package [42] are used for solving the nonlinear optimization formulation.

To guarantee good performance in the convergence process, the proposed TNEP problem is performed in specific steps. Initially, through the optimization technique DE, a random set of solution plans is created considering the specific aspects of the grid, for example, the possibility to include a TCSC between two buses. All solutions of the set are evaluated to verify the operational feasibility and obtain the total investment ν (Eq. (27)), which is used as a deciding element in the selection step of the DE. Subsequently, two operators, named mutation and crossover, are applied to generate new topologies. In the selection step, based on the ν values, all new topologies are compared with the corresponding ones from the previous set. This procedure is repeated until the stopping criterion has been satisfied. Thus, the solution of the updated set with the lowest cost ν is considered as the final plan. The simplified process is illustrated in Fig. 6.

3.4.3. Load shedding

Each possible topology created in the *DE* process is evaluated through the optimization process of the operational problem. This results in different active and reactive load shedding values for each topology, which makes feasible each transmission configuration. Additionally, it can expedite the convergence in situations with or without redispatch. Fictitious generators connected to PQ buses represent the load shedding. Thus, the following scenarios must be understood:

(i) If $\alpha\rho_k > 0$ in the final plan, indicates that at least one constraint has not been satisfied. In this case, fictitious generators generate active power ($\rho_k > 0$), and the cost ν of the current topology increases resulting in a not very attractive transmission configuration.
(ii) If $\beta\varrho_k > 0$ in the final solution, the cost ν increases as a result of reactive power demand to meet the constraints, and the associated buses need reactive power compensation.
(iii) If $\alpha\rho_k = 0$ in the final solution, indicates that the current topology is feasible even without the help of active load shedding.
(iv) If $\beta\varrho_k = 0$ in the final solution, the topology does not need reactive power compensation in the load buses.

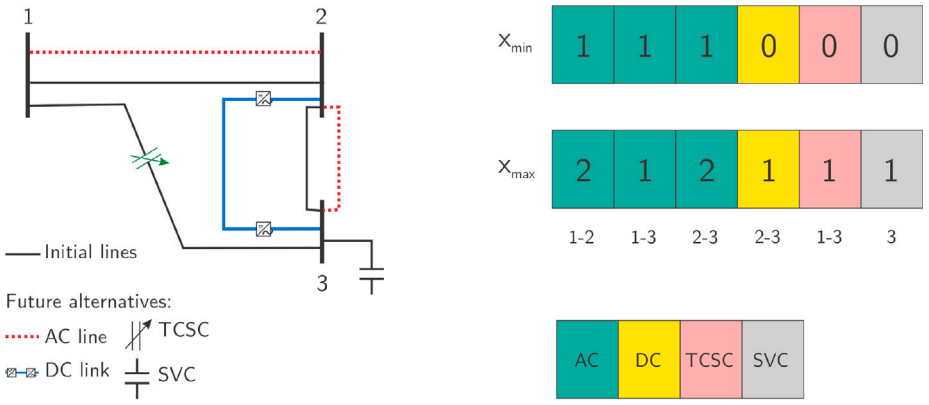

(a) Three buses system. (b) Vectors.

Fig. 5. Example — Three buses system.

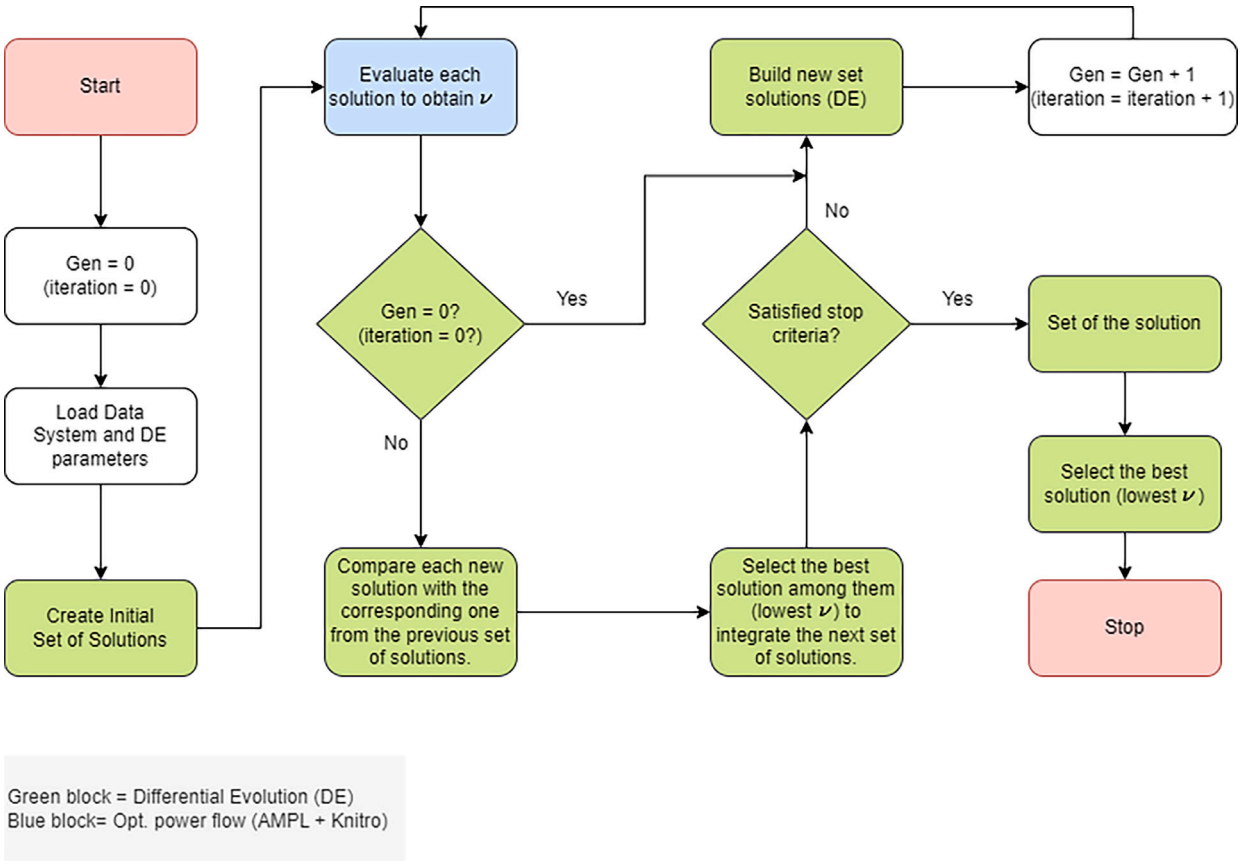

Fig. 6. Flowchart of the proposed solution method.

3.4.4. Stopping criteria

The stopping criteria are a maximum number of iterations (50 for this work), and a non-improved objective function by more than 5% in the last ten iterations.

4. Test and results

A modified version of the WSCC test case (System 1), documented in [43,44], and an IEEE system version with 118 buses (System 2), available in [45,46], are used to test the proposed approach. The base power used in both systems is $|S_{base}| = 100$ MVA. In addition, loads are considered constant power injections.

The initial setup for the DE is 100 possible topologies for System 1 system, and 500 possible topologies for System 2. For both systems the values for α and β are $\$1 \cdot 10^9$/MW and $\$10 \cdot 10^3$/MVAr, respectively. Since active load shedding is not desired, the cost α is set by a high value, forcing the solution method to find a plan where $\rho = 0$.

4.1. Modified WSCC system — System 1

In the base AC topology, 9 AC lines connect the 9 AC buses. The system has three generators and three loads. The SVC at bus 9 is modeled as a reactive power injection, with limits 0.50 pu (upper) and 0 pu (lower). Five buses, four DC lines, and up to four converter stations can form the MTDC system. The MTDC grid can be linked to the AC

Table 2
Generator Data — System 1.

Gen.	Bus No.	Type	P_{min} (pu)	P_{max} (pu)	Q_{min} (pu)	Q_{max} (pu)
Gen1	01	3	0.10	4.00	−4.00	4.00
Gen2	02	2	0.10	4.00	−3.00	4.00
Gen3	03	2	0.10	4.00	−3.00	4.00

Type 3 = Slack; Type 2 = PV.

Table 3
Base case load data — System 1.

Load	Bus No.	P_{load} (pu)	Q_{load} (pu)
Ld1	5	1.90	0.80
Ld2	7	0.50	0.25
Ld3	9	1.25	0.50

Table 4
AC line data — System 1.

Branch name	From bus	To bus	r (pu)	x (pu)	Capacity (pu)	Cost (M$)
BAC1	1	4	0.0000	0.0576	2.00	55
BAC2	4	5	0.0170	0.0920	2.00	40
BAC3	5	6	0.0390	0.1700	2.00	20
BAC4	3	6	0.0000	0.0586	2.00	35
BAC5	6	7	0.0119	0.1008	2.00	60
BAC6	7	8	0.0085	0.0720	2.00	35
BAC7	8	2	0.0000	0.0625	2.00	85
BAC8	8	9	0.0032	0.1610	2.00	40
BAC9	9	4	0.0100	0.0850	2.00	50
[a]BAC10	3	7	0.0390	0.1700	1.50	25
[a]BAC11	2	9	0.0100	0.0850	1.50	65
[a]BAC12	5	1	0.0320	0.1610	1.50	75

[a]New potential AC lines.

Table 5
DC branches — System 1.

Branch path	From bus	To bus	r (pu)	Capacity (pu)	Cost (M$)
BDC1	10	11	0.0073	2.76	20
BDC2	11	14	0.0109	2.76	35
BDC3	14	12	0.0091	2.76	25
BDC4	14	13	0.0065	2.76	30

Table 6
FACTS devices — System 1.

SVC (Bus)	TCSC (Branch)
2	BAC2
5	BAC8
6	BAC9

system at buses 5, 6, 7, and 9 through VSC converters. Refs. [26,27] contain the parameters and data of the VSC stations. The generators and loads data are shown in Tables 2 and 3, respectively.

Tables 4 and 5 show the AC and DC branches data, respectively.

Fig. 7 illustrates the candidate MTDC topology.

Two maximum AC lines are allowed per right-of-way. Each new VSC increases the price of a new DC branch by $50,000. The AC buses and AC branches that can be connected to FACTS devices are shown in Table 6.

The Q_{SVC} limits (in pu) for each SVC are:

$$-0.10 \leq Q_{SVC} \leq 3.50 \quad \text{and}$$

The k_{TCSC} limits are:

$$-0.7 \leq k_{TCSC} \leq 0.2$$

As part of this work, adding a TCSC device and new parallel AC lines to the same branch is not allowed. The results correspond to a 100% of load increase to show the benefits of the proposed model.

Table 7
Results — AC and DC lines allowed.

Branch name	VSC converter AC bus	Total cost (M$)
BAC2, BAC4, BDC1, BDC3, BDC4	5, 6, 7, 9	150.2

Table 8
Results — AC, DC lines and shunt compensation.

New branch	Shunt compensation		Total cost (M$)
	[MVAr]	Bus	
BAC4, BDC3, BDC4	69.7	5	92.52
	26.6	7	
	146.1	9	

Table 9
Results — AC lines, DC lines and FACTS devices.

New branch	FACTS		Total cost (M$)
	Branch TCSC	Bus SVC	
BAC4, BDC3, BDC4	BAC9	4, 5	90.41

(SC1) AC and DC lines allowed

Without grid reinforcements, the system presents limit violations (voltage profile and transmission line capacity). Thus, adding new AC and DC lines is the most viable way to meet all constraints. Table 7 presents the transmission additions and final cost.

In this scenario, AC buses 5–6 are interconnecting through the choice of the BDC3 and BDC4 lines. The BDC1 branch connects the AC buses 7–9. This DC grid consists of 5 new DC buses; however, only 4 VSC converters are installed, since DC bus 14 is not a connection bus to the AC grid. The four installed converters supply reactive power to the AC grid. The DC grid receives active power injection from the AC grid through AC bus 6 and returns it (discounting losses) through AC bus 5. With the new BC4 branch, the generator connected to bus 3 increases the power supply delivered to the system, initially limited to 200 MVA. Two relevant aspects are associated with the MTDC system, namely: (a) increased system transmission capacity and (b) reactive power control through VSC converter stations. Each converter adds an extra cost; nevertheless, this is a more viable strategy to satisfy all constraints.

(SC2) shunt compensation, AC lines, and DC lines

The results show that DC transmission lines additions are not necessary when reactive sources are available, which makes the solution more economical, as depicted in Table 8.

The results reveal that the system presents a voltage limit violation in bus 5, which could be solved by adding converter stations (DC lines) or reactive power sources at similar costs. The SVC injects 50 MVAr of reactive power at bus 9, which is the upper limit for this SVC device.

(SC3) AC and DC lines and FACTS devices

This scenario allows the combination of three alternatives: AC, DC lines, and FACTS devices. SVC devices can be added to buses 1, 4, 5 and 6. TCSC devices can be included at branches BAC2, BAC3, BAC8 and BAC9. Table 9 shows the final additions and cost.

The plan obtained is complementary to the previous scenarios. In other words, the proposed model creates alternatives to meet all operational constraints, mainly in the neighborhood of bus 5. It is interesting to note that the new circuits are the same as in the previous plan, Table 8. However, the FACTS devices produce the same effect as shunt compensation at a lower cost. Thus, the proposed approach proved to be beneficial when all the transmission options are integrated into the same optimization process. Fig. 8 illustrates the expanded system.

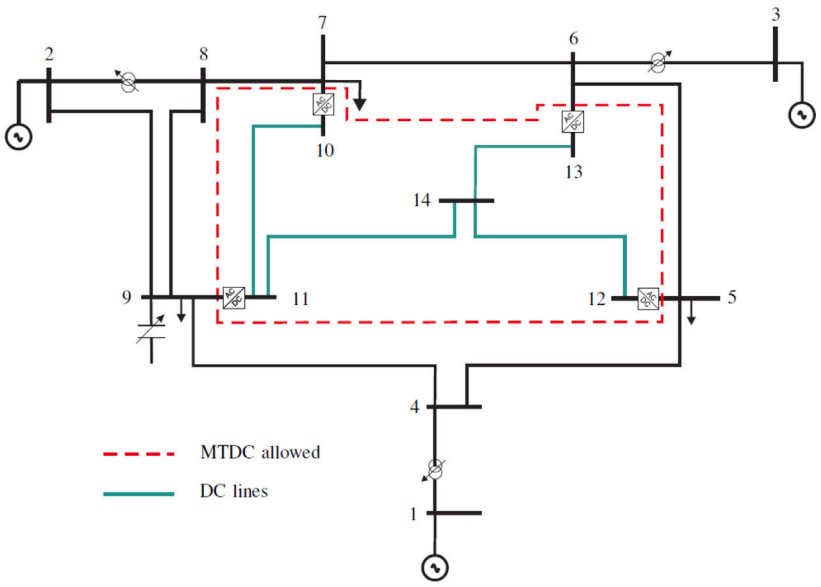

Fig. 7. System 1 — Candidate DC lines.

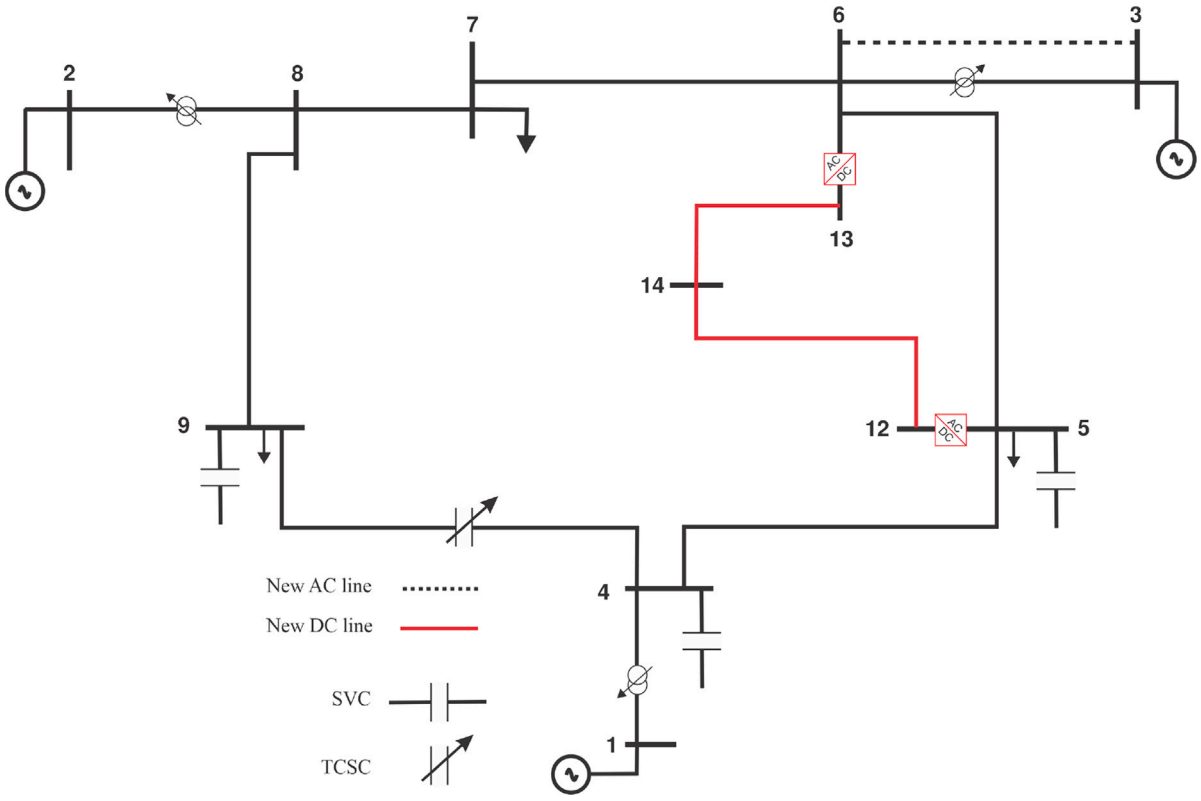

Fig. 8. Final topology — scenario 3.

(SC4) AC/DC lines, FACTS devices and shunt compensation

All possibilities of reinforcements are allowed in this scenario. The results are shown in the Table 10.

The new branch BAC12 and the TCSC connected in series with the branch BAC2, are correlated with the higher load (bus 5). The TCSC improves power transfer capability by regulating BAC2 transmission line reactance. The line BAC12 allows the Gen1 increase in the generation, previously limited by branch BAC1 to 200 MVA. These grid changes lead the Ld1 load to be essentially served by the Gen1. The TCSC in line BAC8 has contributed to supplying the load Ld3. The active

Table 10
Results — AC/DC lines, FACTS devices and shunt compensation.

New branch	FACTS	Shunt Comp.		Total cost (M$)
	Branch TCSC	[MVAr]	Bus	
BAC12	BAC2, BAC8	183.98 65.65 43.93	5 7 9	82.95

Table 11
AC/DC lines allowed — Dispatchable and non-dispatchable generation.

Scenario	Branch	Gen2 (pu)		Gen3 (pu)		Cost M$
		P_g	Q_g	P_g	Q_g	
Dispatchable generation	BAC2, BAC4, BDC1, BDC3, BDC4	1.99	0.01	3.57	0.12	150.2
Non-dispatchable generation	BAC1, BAC3, BAC10, BAC11, BDC2, BDC3	2.0	1.00	2.00	1.00	285.1

Table 12
Output of generation G1.

Scenario	P_g (pu)	Q_g (pu)
Dispatchable generation	1.95	0.15
Non-dispatchable generation (Gen2 and Gen3)	3.51	0,01

Table 13
New CA lines allowed — System 2.

Branch name	From bus	To bus	Branch name	From bus	To bus
BAC3	4	5	BAC4	3	5
BAC14	3	12	BAC30	23	24
BAC44	15	33	BAC45	19	34
BAC54	30	38	BAC99	49	66
BAC106	49	69	BAC115	70	75
BAC127	81	80	BAC140	90	91
BAC149	82	96	BAC159	99	100
BAC176	110	111	BAC180	32	114

load shedding costs present a high value ($\$1 \cdot 10^9$/MW); therefore, the reinforcements' priority is to supply the active power load, considering the minimum investment costs. Thus, to achieve this objective, the result contains shunt compensation. This fact is a direct consequence of the lower reactive load shedding costs ($\$10 \cdot 10^3$/MVAr) compared to the other reinforcements directly related to reactive power, e.g., converter station. The results elucidate the advantage of a flexible model.

(SC5) AC/DC lines with non-dispatchable generation

The proposed approach allows considering dispatchable and non-dispatchable generation. For a non-dispatchable scenario, generators Gen2 and Gen3 were assumed with a fixed generation equal to $P_g = 2$ pu and $Q_g = 1$ pu. Table 11 presents a comparison with scenario *SC1*. This plan is almost 90% more expensive than the one obtained using dispatchable generation. The total active power generation is increased in the Gen1 generator, compensating for the limitations of Gen3, as shown in Table 12. Also, new paths from generators are created to meet the demand. Additionally, the two VSC converters (close to the loads) provide part of the reactive power to the grid, minimizing the generation of reactive power in generator Gen1.

4.2. IEEE 118-bus — System 2

The VSC parameters are the same as those exploited for System 1, including the cost associated with the shunt compensation. However, the installation cost for each new VSC converter for this system was set to M$1. This scenario allows 16 new AC line branches, Table 13, with no more than two lines per right-of-way. The results are obtained for a load 2.5 times higher than its nominal value. The system data are available in the Refs. [45,46]. The costs of the new lines are shown in [46]. The DC data are shown in Table 14.

The Q_{SVC} limits (in pu) for each SVC are:

$$-0.1 \leq Q_{SVC} \leq 3.3$$

The range of k_{TCSC} is:

$$-0.8 \leq k_{TCSC} \leq 0.2$$

Table 14
DC paths for System 2.

Branch path	From AC bus	To AC bus	r (pu)	Capacity (pu)	Cost (M$)
BDC1	27	115	0.005	1.00	8.892
BDC2	32	114	0.005	1.00	7.344
BDC3	30	38	0.005	1.00	6.480
BDC4	49	66	0.005	1.00	11.028
BDC5	49	69	0.005	1.00	32.400
BDC6	83	85	0.005	1.00	17.300

Table 15
Possibilities of FACTS devices.

TCSC — Branch	SVC — Bus
BAC9, BAC18, BAC34, BAC39, BAC66, BAC109	3, 12, 27, 42, 59, 90

Table 15 shows the possible FACTS devices additions to the system.

Two case studies are conducted: (i) allowing all grid reinforcement options and (ii) allowing AC paths, DC links, and shunt compensation. Table 16 presents the final plan for the first case study. The total cost for this plan is M$54.96. The small number of lines (AC or DC) occurs due to the higher cost of lines compared to shunt compensation and FACTS devices costs.

A more expensive solution is obtained by not allowing FACTS devices (second case study), Table 17.

The total shunt compensation investment, and the BDC4 branch make the solution plan more expensive compared to that obtained including FACTS devices, as expected.

Obviously, it is not always necessary to consider all possible alternatives for transmission expansion planning. However, it is interesting to provide a complete model that allows easily extending the planning study to several situations.

The algorithm's robustness is measured by its capability of converging and reaching the same solution for each trial. In this work, ten trials are performed for each test scenario (both systems), and the algorithm always converges and reaches the same solution. Fig. 9 illustrates the convergence process for System 2 (AC-DC lines, shunt compensation, and FACTS devices are allowed), considering 50 interactions as stopping criteria.

Even when it is difficult to compare the results with other approaches due to their differences in the problem formulation, network model, and test systems, it is possible to validate the results through the AC optimal power flow (AC-OPF). For this purpose, the final expansion plans are all feasible. In all the test scenarios, the optimal power flow convergence validated the feasibility of the solutions.

5. Conclusions

There is a need to use a better representation of the network and its elements for the TNEP problem. Although appropriate in several situations, considering only AC and DC circuits options could be not the best mix for expansion, in particular, where the system complexity grows with new system conditions. Thus, this research work proposes a unified AC TNEP model, allowing different types of reinforcements in the same expansion process (AC lines, shunt compensation, FACTS devices, and MTDC system). The results show that the model and approach are promising, allowing greater flexibility in the TNEP process. For example, the installation of an HVDC link creates an alternative power flow route and the VSC converter allows also some reactive power control. Therefore, the formulation is considerably flexible, allowing the TNEP problem to be solved, considering a variety of expansion scenarios. It is also possible to include other device models and consider multistage planning. In addition, the benefits of the proposed approach can include both dispatchable and non-dispatchable generation scenarios. Even when renewable sources are best modeled using uncertainty, the non-dispatchable generation model already creates a very difficult scenario

Table 16
Results System 2 — AC paths, DC links, shunt compensation and FACTS devices.

New line		SVC		TCSC branch		Shunt. Comp.		Total cost (M$)
Branch	VSC AC bus	Bus	Q_{SVC} (pu)	Branch	X_{TCSC} (pu)	Bus	Total Q_{Shunt} (pu)	
BAC30, BDC5	49, 69	3	0.22	BAC34	−0.005	13, 20, 21, 33, 43,	6.67	54.96
		39	0.10	BAC39	−0.020	44, 45, 50, 51, 52,		
				BAC109	−0.053	53, 67, 74, 76, 78, 82, 83, 95, 96, 117, 118		

Table 17
Results System 2 — AC paths, DC links and shunt compensation.

New line		Shunt. Comp.		Total cost (M$)
Branch	VSC AC bus	Bus	Total Q_{Shunt} (pu)	
BAC30, BDC4, BDC5	49, 66, 69	1, 2, 3, 13, 15, 16, 18,19, 20, 21, 22, 33, 34, 35, 36, 43, 44, 45, 49, 50, 51, 52, 53, 57, 58, 59, 66, 67, 74, 76, 78, 79, 84, 95, 96, 117, 118	17.30	72.60

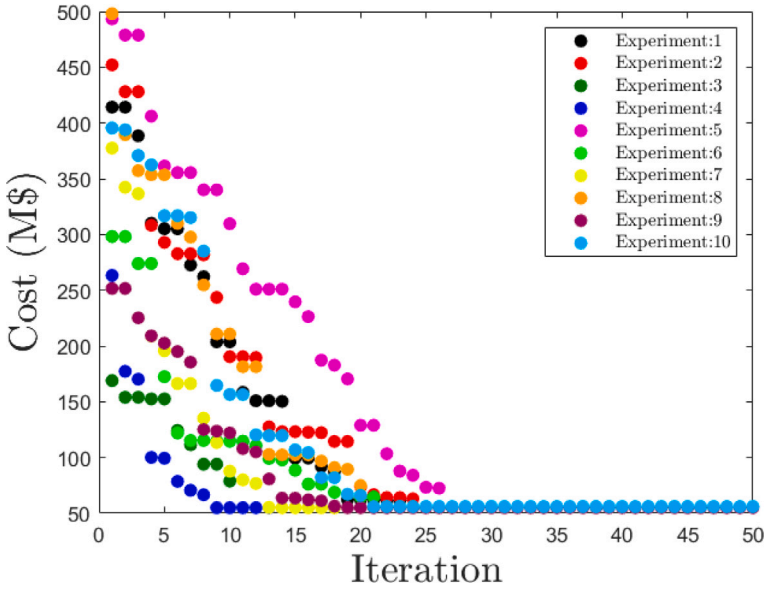

Fig. 9. Convergence process for System 2 (result — Table 16).

to solve. More work should be carried out to consider uncertainty in some TNEP variables and to develop more efficient solution methods for a dynamic TNEP approach.

CRediT authorship contribution statement

Ricardo A. de Araujo: Conceptualization, Methodology, Software, Validation, Formal analysis, Investigation, Writing – original draft. **Santiago P. Torres:** Conceptualization, Methodology, Software, Validation, Formal analysis, Investigation, Writing – original draft. **José Pissolato Filho:** Validation, Formal analysis, Writing – review & editing. **Carlos A. Castro:** Conceptualization, Formal analysis, Investigation, Writing – review & editing. **Dirk Van Hertem:** Conceptualization, Writing – original draft, Writing – review & editing.

Declaration of competing interest

The authors declare that they have no known competing financial interests or personal relationships that could have appeared to influence the work reported in this paper.

Data availability

No data was used for the research described in the article.

References

[1] A. Dini, A. Azarhooshang, S. Pirouzi, M. Norouzi, M. Lehtonen, Security-constrained generation and transmission expansion planning based on optimal bidding in the energy and reserve markets, Electr. Power Syst. Res. 193 (2021) 107017.
[2] H. Hamidpour, J. Aghaei, S. Pirouzi, T. Niknam, A. Nikoobakht, M. Lehtonen, M. Shafie-khah, J.P. Catalão, Coordinated expansion planning problem considering wind farms, energy storage systems and demand response, Energy 239 (2022) 122321.
[3] P. Dersin, New insights in the use of the DC model for steady-state analysis of power systems, in: Proc. 1978 IEEE Conf. on Decision and Control, Incl. 17th Symp. on Adaptive Processes, San Diego/Calif., 1979, pp. 871–877, 1979.
[4] L. Bahiense, G.C. Oliveira, M. Pereira, S. Granville, A mixed integer disjunctive model for transmission network expansion, IEEE Trans. Power Syst. 16 (3) (2001) 560–565.
[5] M. Rahmani, Study of New Mathematical Models for Transmission Expansion Planning Problem (Ph.D. thesis), UNESP, 2013.
[6] H. Hamidpour, S. Pirouzi, S. Safaee, M. Norouzi, M. Lehtonen, Multi-objective resilient-constrained generation and transmission expansion planning against natural disasters, Int. J. Electr. Power Energy Syst. 132 (2021) 107193.
[7] S. Verma, V. Mukherjee, et al., Transmission expansion planning: A review, in: 2016 International Conference on Energy Efficient Technologies for Sustainability (ICEETS), IEEE, 2016, pp. 350–355.
[8] M.A. Farrag, K.M. Ali, S. Omran, AC load flow based model for transmission expansion planning, Electr. Power Syst. Res. 171 (2019) 26–35.
[9] S. Torres, C. Castro, Expansion planning for smart transmission grids using AC model and shunt compensation, Gener. Transm. Distrib. IET 8 (5) (2014) 966–975.

[10] S.P. Torres, C.A. Castro, Specialized differential evolution technique to solve the alternating current model based transmission expansion planning problem, Int. J. Electr. Power Energy Syst. 68 (2015).
[11] A. Lotfjou, Y. Fu, M. Shahidehpour, Hybrid AC/DC transmission expansion planning, IEEE Trans. Power Deliv. 27 (3) (2012) 1620–1628.
[12] A. Arabpour, M.R. Besmi, P. Maghouli, Transmission expansion and reactive power planning considering wind energy investment using a linearized AC model, J. Electr. Eng. Technol. 14 (3) (2019) 1035–1043.
[13] P.A. Bhattiprolu, A.J. Conejo, Multi-period AC/DC transmission expansion planning including shunt compensation, IEEE Trans. Power Syst. 37 (3) (2022) 2164–2176.
[14] K. Soleimani, J. Mazloum, Considering facts in optimal transmission expansion planning, Eng. Technol. Appl. Sci. Res. 7 (5) (2017).
[15] J. Dave, H. Ergun, T. An, J. Lu, D. Van Hertem, TNEP of meshed HVDC grids: 'AC', 'DC' and convex formulations, IET Gener. Transm. Distrib. 13 (24) (2019) 5523–5532.
[16] M. Moradi-Sepahvand, T. Amraee, Hybrid AC/DC transmission expansion planning considering HVAC to HVDC conversion under renewable penetration, IEEE Trans. Power Syst. 36 (1) (2020) 579–591.
[17] J. Dave, H. Ergun, D. Van Hertem, Relaxations and approximations of HVdc grid TNEP problem, Electr. Power Syst. Res. 192 (2021) 106683.
[18] Y. Wen, Y. Lu, J. Gou, F. Liu, Q. Tang, R. Wang, Robust transmission expansion planning of ultrahigh-voltage AC–DC hybrid grids, IEEE Trans. Ind. Appl. 58 (3) (2022) 3294–3302.
[19] A.H. Dominguez, L.H. Macedo, A.H. Escobar, R. Romero, Multistage security-constrained HVAC/HVDC transmission expansion planning with a reduced search space, IEEE Trans. Power Syst. 32 (6) (2017) 4805–4817.
[20] H. Doagou-Mojarrad, H. Rastegar, G.B. Gharehpetian, Probabilistic multi-objective HVDC/AC transmission expansion planning considering distant wind/solar farms, IET Sci. Meas. Technol. 10 (2) (2016).
[21] A.A. Ghadimi, M. Amani, M. Bayat, S. Ahmadi, M.R. Miveh, F. Jurado, Stochastic transmission expansion planning in the presence of wind farms considering reliability and N-1 contingency using grey wolf optimization technique, Electr. Eng. 104 (2) (2022) 727–740.
[22] X. Zhang, K. Tomsovic, A. Dimitrovski, Security constrained multi-stage transmission expansion planning considering a continuously variable series reactor, IEEE Trans. Power Syst. 32 (6) (2017) 4442–4450.
[23] J. Zhu, Optimization of Power System Operation, in: IEEE Press Series on Power Engineering, Wiley, 2009.
[24] J. Arrillaga, C. Arnold, Computer Analysis of Power Systems, Wiley, 1990.
[25] M. Davies, M. Dommaschk, J. Dorn, J. Lang, D. Retzmann, D. Soerangr, HVDC PLUS - Basics and Principle of Operation, Tech. Rep., Siemens, 2008, URL http://www.energy.siemens.com.
[26] J. Beerten, S. Cole, R. Belmans, A sequential AC/DC power flow algorithm for networks containing multi-terminal VSC HVDC systems, in: Power and Energy Society General Meeting, 2010 IEEE, 2010, pp. 1–7.
[27] W. Feng, A.L. Tuan, L. Tjernberg, A. Mannikoff, A. Bergman, A new approach for benefit evaluation of multiterminal VSC-HVDC using a proposed mixed AC/DC optimal power flow, IEEE Trans. Power Deliv. 29 (1) (2014).
[28] R. Mathur, R. Varma, Thyristor-Based FACTS Controllers for Electrical Transmission Systems, in: IEEE Press Series on Power Engineering, Wiley, 2002.
[29] K. Keerthivasan, V. Deve, J. Jerome, R. Ramanujam, Modeling of SVC and TCSC for power system dynamic simulation, in: 2005 International Power Engineering Conference, 2005, pp. 696–700 Vol. 2.
[30] M. Basu, Multi-objective optimal power flow with FACTS devices, Energy Convers. Manage. 52 (2) (2011) 903–910.
[31] S. Varma, FACTS devices for stability enhancements, in: 2015 International Conference on Green Computing and Internet of Things (ICGCIoT), 2015, pp. 69–74.
[32] V. Suresh, S. S., Performance comparison of SVC and TCSC in power flow control, in: 2015 International Conference on Computer Communication and Informatics (ICCCI), 2015, pp. 1–5.
[33] N. Hingorani, L. Gyugyi, Understanding FACTS: Concepts and Technology of Flexible AC Transmission Systems, Wiley, 2000.
[34] L.J. Cai, I. Erlich, G. Stamtsis, Optimal choice and allocation of FACTS devices in deregulated electricity market using genetic algorithms, in: IEEE PES Power Systems Conference and Exposition, 2004, 2004, pp. 201–207, vol.1.
[35] H.R. Baghaee, B. Vahidi, S. Jazebi, G.B. Gharehpetian, A. Kashefi, Power system security improvement by using differential evolution algorithm based FACTS allocation, in: 2008 Joint International Conference on Power System Technology and IEEE Power India Conference, 2008, pp. 1–6.
[36] M. Sepesy Maucec, J. Brest, B. Boskovic., Z. kacic, Improved differential evolution for large-scale Black-Box optimization, IEEE Access 6 (2018) 29516–29531.
[37] A. Glotić, A. Glotić, P. Kitak, J. Pihler, I. Tičar, Parallel self-adaptive differential evolution algorithm for solving short-term hydro scheduling problem, IEEE Trans. Power Syst. 29 (5) (2014) 2347–2358.
[38] C. Bu, W. Luo, T. Zhu, R. Yi, B. Yang, Species and memory enhanced differential evolution for optimal power flow under double-sided uncertainties, IEEE Trans. Sustain. Comput. (2019) 1.
[39] S. Torres, R. de Araujo, C. Castro, J. Pissolato, Security constrained transmission expansion planning for smart transmission grids based on the AC network model, in: Transmission Distribution Conference and Exposition - Latin America (PES T D-la), 2014 IEEE PES, 2014, pp. 1–6.
[40] MATLAB, R2019b, The MathWorks Inc, 2019.
[41] R. Fourer, D. Gay, B. Kernighan, AMPL: A Modeling Language for Mathematical Programming, Thomson/Brooks/Cole, 2003.
[42] KNITRO - Nonlinear optimization solver, URL http://www.artelys.com/.
[43] WSCC 9-Bus SystemData [link]. URL http://icseg.iti.illinois.edu/wscc-9-bus-system/.
[44] V. Saplamidis, R. Wiget, G. Andersson, Security constrained optimal power flow for mixed AC and multi-terminal HVDC grids, in: PowerTech, 2015 IEEE Eindhoven, 2015, pp. 1–6.
[45] IEEE 118-bus SystemData. [link]. URL http://motor.ece.iit.edu/Data/Gastranssmion_118_14test.xls.
[46] R.A. de Araujo, Transmission Expansion Planning using AC Model and Considering HVDC, FACTS Devices and Shunt Compensation (Ph.D. thesis), 2017, pp. 92–106.